Cancer Chemother Pharmacol (1996) 37: 547–555

ORIGINAL ARTICLE

**Michael Belanich · Terri Randall · Monica A. Pastor
Jeannie T. Kibitel · Lori Green Alas · M. Eileen Dolan
S. Clifford Schold Jr · Marc Gander
Ferdy J. Lejeune · Benjamin F.L. Li · Agnes B. White
Patricia Wasserman · Marc L. Citron · Daniel B. Yarosh**

Intracellular localization and intercellular heterogeneity of the human DNA repair protein O^6-methylguanine-DNA methyltransferase

Received: 18 March 1995/Accepted: 6 July 1995

Abstract O^6-Methylguanine-DNA methyltransferase (MGMT) is a DNA repair protein that removes alkyl adducts from DNA and may be important in tumor resistance to alkylation chemotherapy. MGMT was visualized in human cells and tumor tissues with monoclonal antibodies against MGMT and immunofluorescence microscopy, and fluorescent signals were quantified by digital image analysis. MGMT was found both in the cytoplasm and the nucleus, and in either locale the protein reacts with alkylated DNA bases and becomes inactivated and lost from the cell. Cell lines in culture and xenografts showed a broad normal distribution of nuclear MGMT levels, but human brain tumors often showed a skewed distribution, with a significant fraction of cells with high levels of MGMT. O^6-Benzylguanine, a suicide substrate inactivator for MGMT activity, reduced MGMT in human cells and in a mouse xenograft to levels undetectable by antibody assay 1 h post-treatment. In melanoma specimens taken from a patient 3 h post-treatment with temozolomide, MGMT levels were reduced by 70%. This quantitative immunofluorescence assay can be used to monitor MGMT and its depletion in human tumors to improve the use of alkylating agents in cancer chemotherapy.

Key words Alkyltransferase · 1,3-Bis(2-chlorethyl)-1-nitrosourea · Carmustine · O^6-Benzylguanine · temozolomide

Abbreviations *MGMT* O^6-Methylguanine-DNA methyltransferase · *BCNU* 1,3-bis(2-chloroethyl)-1-nitrosourea · *O^6-bGua* O^6-benzylguanine · M_{ab}, monoclonal antibodies · *QIF* quantitative immunofluorescence · *IGV* integrated gray value · *Mer^-* methyl repair deficient · *PBS* phosphate-buffered saline · *FITC* fluorescein isothiocyanate · *DAPI* 4′,6-diamidino-2-phenylindole · *CCD* charged coupled device

M. Belanich (✉) · T. Randall · M.A. Pastor · J.T. Kibitel
L.G. Alas · D.B. Yarosh
Applied Genetics Inc., 205 Buffalo Ave, Freeport NY 11520, USA

M.E. Dolan
Section of Hematology-Oncology, The University of Chicago, Chicago, IL 60637-1470, USA

S.C. Schold
Department of Neurology, Southwestern Medical Center, Dallas, TX 75235–9036, USA

M. Gander, F.J. Lejeune
Centre Pluridisciplinaire D'Oncologie, Centre Hospitalier, Universitaire Vaudois, CH-1011 Lausanne, Switzerland

B.F.L. Li
Institute of Molecular and Cell Biology, National University of Singapore, Singapore 0511

A.B. White, P. Wasserman, M.L. Citron
Medical Oncology, Long Island Jewish Medical Center, New Hyde Park, NY 110 42, USA

Introduction

O^6-Methylguanine-DNA methyltransferase (MGMT) is a DNA repair protein which transfers and accepts alkyl groups from the O^6 position of guanine, and inactivates itself upon the repair of the DNA [16]. MGMT is probably important both in the initial treatment of cancer with nitrosourea-based alkylation chemotherapy (such as BCNU and temozolomide) and in the subsequent development of drug resistance. Human tumors show a wide inter-individual variation in MGMT activity [5] that is paralleled by MGMT mRNA levels [6]. Human tumors deficient in MGMT (Mer^-), are extremely sensitive to treatment with alkylating agents such as BCNU when grown as xenografts in mice [18]. Understanding resistance factors in alkylation chemotherapy may enhance the use of new agents, such as temozolomide for brain cancer [15],

and O^6-benzylguanine (O^6-bGua), a suicide substrate for MGMT and therefore a potent biological modulator [7].

To date, measurement of MGMT has relied on biochemical activity assays or mRNA analyses of cell extracts. While these assays measure the average of all cells contributing to the extract, they do not provide information about the intracellular distribution (cytoplasmic versus nuclear) nor the intercellular heterogeneity (tumor cell population distribution) of MGMT protein in the sample, which may be important in understanding how MGMT contributes to drug resistance. One approach to garnering such data is staining human tumor sections with monoclonal antibodies (Mabs) against MGMT and quantifying the amount of bound antibody. We developed a quantitative immunofluorescent (QIF) assay using such antibodies and a computerized image analysis system [3]. We used this method to examine the intracellular distribution of MGMT and to measure the heterogeneity of MGMT in tumor cell cultures and primary tumor samples.

Materials and methods

Monoclonal antibodies

M_{ab} 3B8 was raised against recombinant human MGMT as described by Ayi *et al.* [2]. M_{ab} NFC2 was raised against purified active recombinant human MGMT as follows: Human recombinant MGMT was purified [19], assayed for activity and linked to keyhole limpet hemocyanin (Pierce, Rockford, Ill). BALB/c mice (Charles River Labs, Charles River, Mass.) were inoculated i.p. with a mix of antigen and Freund's complete adjuvant (Sigma, St. Louis, Mo.) and boosted 8 times with a mix of antigen and incomplete Freund's adjuvant. Spleen cells were fused to FO myeloma cells (American Type Culture Collection, Bethesda, Md.) and hybridomas were screened by ELISA using purified active MGMT. Subclones were grown in PFHMII protein-free hybridoma medium (Gibco, Gaithersburg, Md.).

The M_{ab} 3B8 is specific for human MGMT by several criteria: (1) it stains a 21 kDa band in western blots of Mer^+ cells; (2) it does not stain such a band in western blots of Mer^- cells; and (3) its staining in western blots of Mer^+ cells is abolished by treating the cells with the MGMT-specific inhibitor O^6bGua [3]. M_{ab} NFC2 immunoprecipitates MGMT recognized by M_{ab} 3B8, and, in immunohistochemistry, its binding to Mer^+ cells is depleted by pretreatment of cells with O^6-bGua (data not shown). These antibodies recognize methylated MGMT *in vitro* by ELISA, and the loss of staining in cells in which the MGMT is alkylated is due to the proteolytic degradation of the alkylated form of MGMT [3, 16]. The optimum M_{ab} 3B8 concentration of 34 μg/ml for immunostaining was determined by using a range of concentrations on HT29 cells spotted on slides. NFC2 antibody was used at a concentration of 30 μg/ml in the protein-free cell culture supernatant.

Immunofluorescent staining

Cells in culture

Human tumor cells were cultured in Dulbecco's modified Eagle's medium (Gibco, Gaithersburg, Md.) with 10% newborn calf serum (Irving Scientific, Irving, Calif.) and antibiotics, as described [20]. O^6-bGua (a gift of R. Moschel, National Cancer Institute) (10 mm in DMSO) was diluted to 25 μm into cell culture media immediately before use. The cells were grown to 80% confluence on chamber slides (Nunc, Naperville, Ill.), washed with PBS and fixed in 4% paraformaldehyde/PBS for 10 min.

Xenograft tumors

Human lung tumor line A549 and brain tumor line SF767 were grown in NIH Swiss athymic mice at the University of Chicago. Xenografts of human rhabdomyosarcoma cell line TE-671 (H-217) were grown in nude BALB/c athymic mouse hosts at the Southwest Medical Center [18]. O^6-bGua in cremophor was administered to rabdomyosarcoma xenograft hosts as a 90-mg/m^2 i.p. injection and tumors were excised 0.5, 1, 2, 4, 6, 12, and 24 h post-treatment, flash frozen, and cryosectioned. Animal studies were performed according to the guidelines described in "Principles of Laboratory Animal Care" (NIH publication No. 85–23).

Human tumors

Frozen sections of melanoma tumors were obtained at the Centre Pluridiscipinaire d'Oncologie in Lausanne from subcutaneous skin metastases which developed 2 years after treatment of the primary tumor. Two metastases from the same patient were biopsied; one 3 days before treatment and one 3 h after administration of 250 mg/m^2 temozolomide ([5,1-d]1,2,3,5-tetrazin-4(3H)-one), supplied by the Centre under an experimental protocol) as a 1-h i.v. injection. Informed consent was obtained from the patient before treatment.

Thirty-one glioblastoma multiforme tumors (WHO grade IV) were fixed in formalin overnight, embedded in paraffin, and sectioned at Long Island Jewish Medical Center (New Hyde Park, N.Y.). The diagnoses were verified by pathology examination according to the WHO Classification System [12] and sections with high tumor content were selected for QIF analysis.

QSCM standards

Quantum Simply Cellular Microbeads (Flow Cytometry Standards, Hato Rey, Puerto Rico), a set of five microbeads with different amounts of goat anti-mouse antibody bound to their surface, were stained in parallel during all QIF analyses. Approximately 50 μl (2×10^6 particles per ml) of each microbead suspension was placed on individual microscope slides treated with poly-L-lysine (Sigma, St. Louis, Mo.) and allowed to dry. All subsequent manipulations, including fixation, blocking and immunochemical staining, were performed in parallel with the sample.

General staining procedure

All histological and cytological slide preparations were stored frozen until processed for QIF analysis. In a test of slide preservation at −70, −20, 4, and 25°C, we found that storage of cryostat sections or paraffin block sections of A549 and SF767 xenograft tumors at temperatures greater than 4°C for 2 weeks raised nonspecific staining and obscured analysis of MGMT-specific staining (data not shown).

Thawed tissue sections or cells in culture were fixed with 4% paraformaldehyde/PBS at 25°C for 10 min, permeabilized with 0.1% Triton X-100/PBS and blocked with 5% nonfat milk/PBS. Slides were then incubated for 1 h at room temperature with

primary antibody (34 μg/ml M_{ab} 3B8 in block or M_{ab} NFC2 hybridoma supernatant at 30 μg/ml mouse IgG), washed with 0.1% Triton X-100/PBS, incubated for 1 h with FITC-conjugated goat anti-mouse antibody (Sigma, St. Louis, Mo.) in block and washed with 0.1% Triton X-100/PBS. DAPI was added at 0.5 μg/ml for 3 min followed by three washes in deionized H_2O. Slides were mounted in 50% glycerol with Slowfade antifade agent (Molecular Probes, Eugene, Ore.).

Image Analysis

Image acquisition

Epifluorescence microscopy was performed with a Nikon Diaphot microscope equipped with a B-2A filter cube (450– to 490-nm excitation filter, 520-nm barrier filter, 510-nm dichroic mirror) and a UV-2A filter cube (330– to 380-nm excitation, 420-nm barrier filter, 400-nm dichroic mirror) (Nikon, Garden City, N.Y.). Fluorite objective lenses were used to maximize fluorescence imaging (Nikon, Garden City, N.Y.). Digital images were acquired with a Star I cooled CCD camera system (Photometrics, Tucson, Ariz.). A DAPI and FITC image were taken of each field using the UV-2A and B-2A filter sets, respectively. All images were retrieved using a 40× objective; final magnification of the digitized image was 1300×.

The extent of photobleaching by direct and nearby illumination was measured in HT29 cells stained with M_{ab} 3B8 and mounted with Slowfade antifade agent (Molecular Probes, Eugene, Ore.). The average time a field was illuminated during focusing and exposure was 30 s. Directly illuminating a field for 30 s prior to beginning the image collection reduced the fluorescence by only 11% compared to beginning image collection immediately, a statistically insignificant difference. Routine specimen handling exposed the tissue to approximately 4 min of total illumination. Illumination one field for 4 min reduced the fluorescence in another field 5 mm away by only 3% compared to not illuminating a nearby field, a statistically insignificant difference. Thus, photobleaching during routine handling and image acquisition was negligible.

Data collection

Digital images were analyzed with the Optimas image analysis software package (Bioscan, Edmonds, Wash.) using a customized program that automates data collection and performs all calculations. To analyze a field of cells, first the DAPI image was retrieved and nuclei were delineated, then the nuclear outline was superimposed on the FITC image, and finally the fluorescence intensity and area of each nucleus were calculated.

Calculations and definitions

IGV: The sum of all gray scale values within a selected nuclear area
IGV_{Area}: IGV divided by area (fluorescence intensity).
Uncorrected molecules per nucleus: IGV_{Area} of a nucleus divided by the slope of the microbead standard regression multiplied by the area. The microbead standards were used to calibrate the intensity of the nuclear staining, and the total molecules per nucleus was determined by multiplying the molecules per area by the nuclear area. The slope of the linear regression between the IGV_{Area} and the computed molecules divided by the area of the bead standards provides a relationship between fluorescent intensity and the density of bound FITC molecules [3]. Preparations with excessive non-specific staining and autofluorescence were identified by frequency distribution analysis. This occurs when the variance of the background distribution is greater than that in the foreground, or when the background mean is significantly higher by *t*-test than the foreground mean.
Molecules per nucleus: Molecules per nucleus represent the difference between average MGMT-specific uncorrected molecules per nucleus and average background uncorrected molecules per nucleus (see below). If the difference was not statistically significant by *t*-test ($P > 0.05$) then MGMT was not detected (Mer^-).
Percent outliers: The number of cells that had molecules per nucleus values equal or greater than 2.4 standard deviates above the average molecules per nucleus of the same tissue stained with secondary antibody only. Outliers represent cells with signals that have a less than 1% chance of being background.

Background evaluation

Background fluorescence is a combination of intrinsic autofluorescence of the tissue and non-specific binding of the secondary antibody. We obtained background fluorescence information from control slides of the same tissue stained as described above with primary antibody omitted. The results with omission of primary antibody are no different from incubation with isotype antibody from myeloma line MOPC (data not shown). The control slides were closely matched to the experimental slides since control slides were selected from the same set of serial sections as the experimental slides.

Image acquisition and analysis were performed on the control slides as described above and we calculated the number of uncorrected molecules per nucleus caused by background non-specific fluorescence of a population of cells. From the population distribution of background uncorrected molecules per nucleus we determined if the background was too high to quantitate images from slides stained with MGMT-specific antibody. Background fluorescence obscured the MGMT-specific signal when the average or variance of the uncorrected molecules per nucleus measurements for the control slide were significantly greater ($P < 0.05$, by *t*-test or *f*-test, respectively) than the MGMT-specific measurements.

MGMT activity assay

MGMT activity was assayed as described by Citron *et al.* [5]. Briefly, cells were washed with PBS, sonicated, centrifuged at low speed to remove particulate matter, and dialyzed overnight against assay buffer. The protein and DNA concentration of the extract were measured by the Bradford assay (Bio-Rad, Richmond, Calif.) and TK100 fluorimetry (Hoefer Scientific Instruments, San Francisco, Calif.), respectively. Either 250 μg or 500 μg of protein from each extract was incubated with O^6-[^{3}H-methyl]guanine-DNA. After the reaction, the amount of radiolabeled methyl groups transferred from DNA to the collected protein was used to calculate the MGMT activity. For each sample, MGMT activity was measured at two protein concentrations in each assay and each assay was performed in duplicate. The MGMT activity measures were averaged to determine the value for each sample.

Enucleation

T98G brain tumor cells were grown on 2-cm^2 glass slides coated with poly-L-lysine until greater than 80% confluent. Fresh medium containing 20 μg/ml cytochalasin B (Sigma, St. Louis, Mo.) was added and incubated for 90 min at 37°C. Each slide was inverted and placed in a 30-ml Corex tube (cells facing the bottom of the tube) containing 2 ml of medium with 20 μg/ml cytochalasin B. The tubes were centrifuged in a fixed angle rotor at 10 000 × *g* for 15 min at 34°C. Slides were removed from tubes, placed in culture dishes, washed 3 times with cytochalasin-free medium and allowed to recover for 2 h at 37°C. Cells were stained by the standard

immunostaining protocol. Slides treated with O^6-bGua (25 μm) were exposed to O^6-bGua throughout treatment, including the 2-h recovery period after enucleation.

Results

Intracellular localization of MGMT

The intracellular localization of MGMT was examined by immunofluorescence staining with MGMT-specific M_{ab}s of cells in culture and histological and cytological preparations of tumors. M_{ab}s 3B8 and NFC2, which were both raised against native active MGMT, showed nuclear and cytoplasmic staining, and the proportions of nuclear and cytoplasmic staining varied among cell types. Figure 1A and B are DAPI-stained and MGMT-specific M_{ab} 3B8-stained FITC images of a T98G glioblastoma cell. MGMT is prevalent in the nucleus but a substantial amount of MGMT was in the cytoplasm. The proportion of nuclear and cytoplasmic staining often varied within a population of cells, as is apparent in Fig. 1D. Here, the upper portion of the M_{ab}-stained field contains a cluster of HT29 cells with predominantly cytoplasmic staining and, immediately below these cells, is a cluster of cells with predominantly nuclear staining. Histological preparations from a glioblastoma multiforme brain tumor stained with M_{ab} 3B8 showed mainly cytoplasmic staining (Fig. 1F). In contrast, a preparation from an infiltrating ductal breast tumor showed distinct nuclear staining (Fig. 1H).

Since MGMT is a DNA repair protein, the presence of cytoplasmic MGMT was unexpected. However, the size of the MGMT protein (21 kDa) might allow the protein to passively diffuse through nuclear pores. By measuring MGMT in enucleated cells (cytoplasts), we determined the proportion of MGMT in the cytoplasm. Enucleation was limited to no more than half of the cells on a slide, which allowed the quantitation of nuclei (cells that failed enucleation) on the same slide as cytoplasts.

Cells that failed enucleation appeared similar to untreated cells; both the nucleus and cytoplasm fluoresced and the greatest intensity was in the nucleus (compare untreated cell in Fig. 1B with lower cell on Fig. 2A). Cytoplasts also fluoresced, but with less intensity (Fig. 2A). Quantitation of these fluorescent signals indicates that 72 ± 4% of MGMT was within the nucleus (50 nuclei scored) while 28 ± 6% was in the cytoplasm (62 cytoplasts scored). MGMT was not above background in either cytoplasts or nuclei when O^6-bGua (25 μm) was added to the media to deplete MGMT (Fig. 2D), confirming the MGMT specificity of the fluorescent staining.

Although a substantial fraction of MGMT was within the cytoplasm, its significance is not known. In this study we focused our QIF analysis on MGMT in the nucleus because the nucleus was easily delineated by staining with DAPI, a chromatin-specific fluorescent dye. Therefore, the nuclear fluorescence serves as a surrogate measure for total MGMT in the cell. We found that nuclear MGMT correlated with MGMT

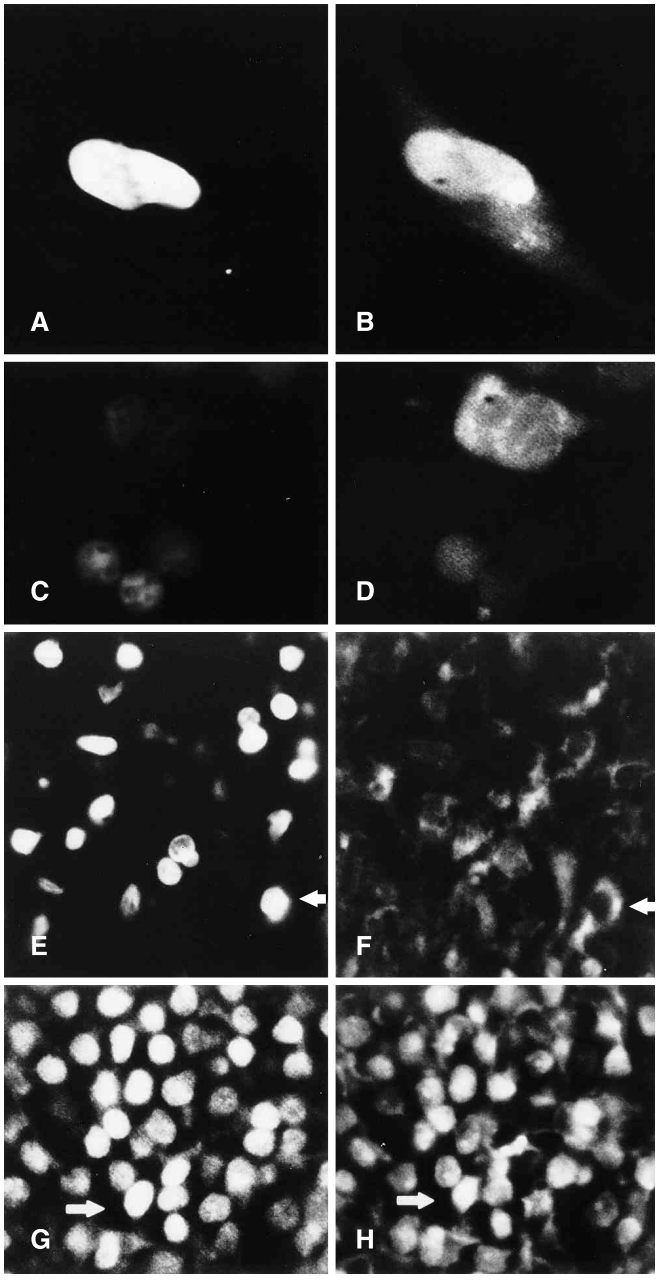

Fig. 1A–H Digital images of human cells stained with O^6-methylguanine-DNA methyltransferase (MGMT)-specific monoclonal antibody (M_{ab}) 3B8 using fluoroscein isothiocyanate (FITC)-conjugated secondary antibody and corresponding 4′,6′-diamilino-2-phenyl indole (DAPI) staining (nuclei). **A**, **B** T98G glioblastoma cells, DAPI and MGMT. **C**, **D** HT29 colon cancer cells, DAPI and MGMT. **E**, **F** Paraffin-embedded, formalin-fixed glioblastoma tumor, DAPI and MGMT. **G**, **H** Paraffin-embedded, formalin-fixed malignant breast tumor (infiltrating duct carcinoma), DAPI and MGMT

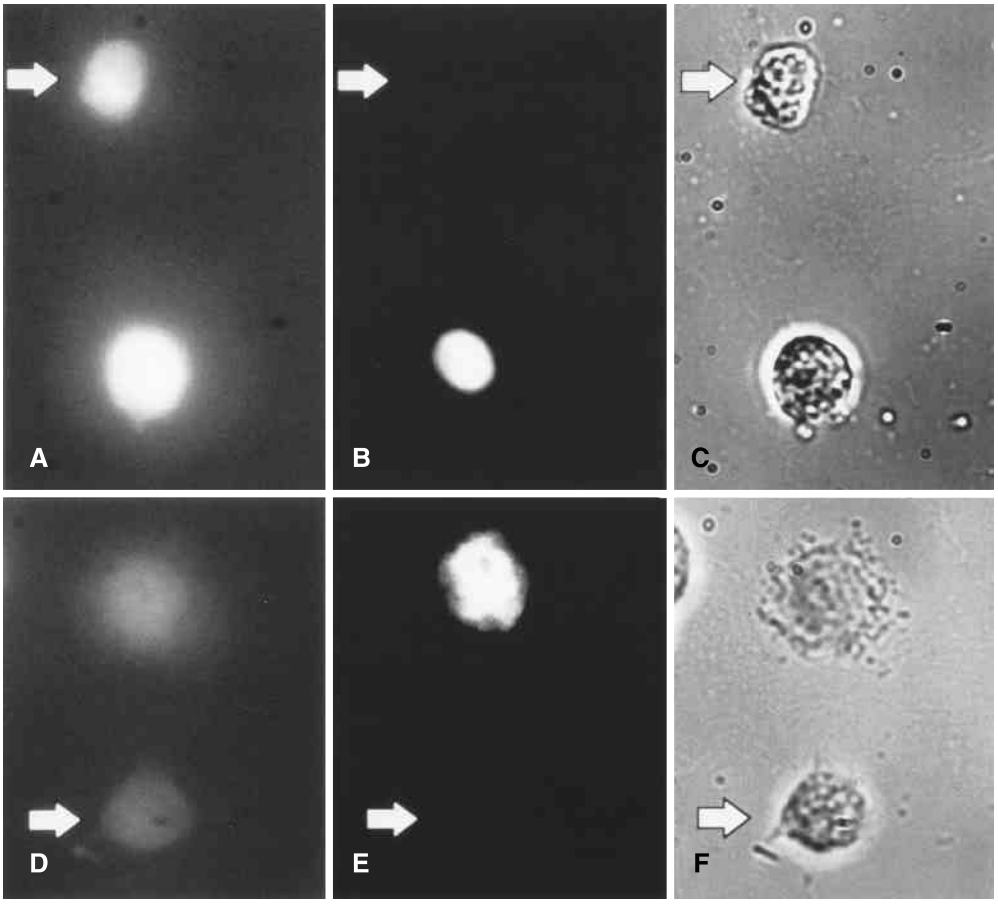

Fig. 2A–F T98G glioblastoma cytoplasts stained with MGMT-specific M_{ab} 3B8 with FITC-conjugated secondary antibody and DAPI. **A**–**C** MGMT, DAPI, and bright field images of T98G cytoplast (*arrow*) and a nucleated cell. **D**–**F** MGMT, DAPI, and bright fields images of T98G cytoplast (*arrow*) and nucleated cell treated with 25 μm O^6-benzylguanine (O^6-bGua)

biochemical activity in tumor cells. Figure 3 shows a comparison between MGMT content, measured by immunofluorescence staining, and activity. The average immunofluorescence in the population of cells was quantified by total IGV or molecules per nucleus. Activity measurements correlated with both immunofluorescence quantitation methods, but the absolute values were nearly an order of magnitude greater in the QIF assay.

Intercellular heterogeneity of MGMT

The QIF method provides information on the MGMT distribution within a population by measuring individual cells. The intercellular frequency distribution of MGMT content within a specimen may reveal a small population of cells with high MGMT content, which would be missed in an average measurement. Clonal populations of tissue culture cells, such as U87MG and T98G, have normal frequency distributions (Fig. 4, top), as do rhabdomyosarcoma cells grown as xenografts (data not shown). Similar distributions were found in 7 of 31 glioblastoma tumors, an example of which is shown in Fig. 4 (center panel). However, the remaining 24 tumors had a skewed distribution, often with a population of cells with significantly greater molecules per nucleus, an example of which is shown in Figure 4 (bottom panel).

These skewed distributions may indicate that human tumors are composed of subpopulations of cells, each expressing a different level of MGMT. To model this situation we seeded different proportions of Mer^+ T98G glioblastoma cells and Mer^- U87MG glioblastoma cells onto chamber slides and measured MGMT content by QIF using M_{ab} 3B8. The correlation between the percentage of Mer^+ seeded and percentage of outliers is shown in Fig. 5. As expected, the average molecules per nucleus also increased with the percentage of Mer^+ seeded. These results show that the QIF assay can measure not only the average MGMT level in a tumor cell population, but also measure subpopulations expressing high levels of MGMT. In a majority of the brain tumors examined (24/31) these subpopulations were clearly detectable as outliers above the 1% frequency found in normally distributed populations.

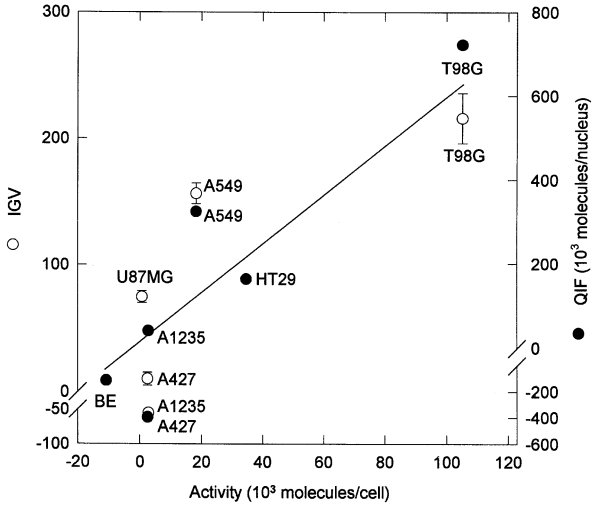

Fig. 3 Quantitative immunofluorescence (*QIF*) measurements of MGMT-specific staining with M_{ab} 3B8 compared with biochemical MGMT activity measurements of seven tumor cell lines. Mer^+ (methyl repair competent) cell lines and number of nuclei examined by QIF in *parenthesis*: T98G (53), HT29 (26), and A549 (82); Mer^- (methyl repair deficient) cells and number of nuclei examined by QIF in *parenthesis*: U87MG (87), A1235 (54), A427 (32), and BE (21). *Abscissa* MGMT biochemical activity; *ordinate* QIF measured in two experiments: *open circles* are total integrated gray value (*IGV*), a measure of the fluorescence of the nuclei, (correlation coefficient 0.595); *filled circles* are molecules per nucleus, which is the nuclear fluorescence converted to molecules per cell using the microbead standards (correlation coefficient 0.735)

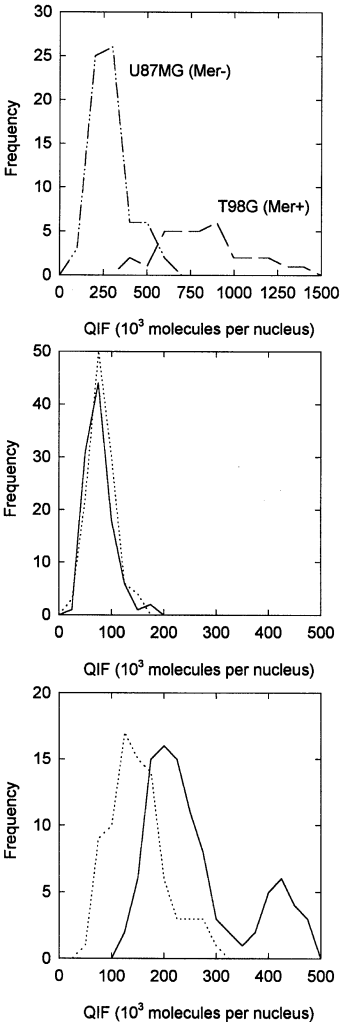

Fig. 4 Intercellular heterogeneity of MGMT quantitated by QIF. *Top* Brain tumor cell lines U87MG (Mer^- 68 nuclei scored) and T98G (Mer^+, 32 nuclei scored). *Middle* and *bottom Solid line* is MGMT-specific foreground staining with Mab 3B8, *dotted line* is background fluorescence. *Middle* Glioblastoma tumors with 0% outliers (103 nuclei scored for foreground, 115 nuclei scored for background). *Bottom* The 29% outliers (49 nuclei scored for foreground, 50 nuclei scored for background)

O^6-bGua depletion can be measured in xenograft tumors

O^6-bGua is a suicide inhibitor of MGMT activity. We have previously shown that O^6-bGua treatment of cells in culture reduces antibody binding [3], and we tested the ability of the antibody assay to detect depletion in human tumors grown as xenografts in mice. BALB/c nude mice were inoculated with human rhabdomyosarcoma cell line TE-671 (H-271), a line with moderately high levels of MGMT. Xenograft hosts were treated with 90 mg/m^2 O^6-bGua in cremophor administered i.p. and tumors were excised at 0.5, 1, 4, 6, 12, and 24 h post-treatment, sectioned, and stained with antibodies against human MGMT. MGMT was detected in untreated tumors, but 1 h post-treatment MGMT was undetectable and remained low for 24 h (Fig. 6). The anomalously high value at 12 h was due to a single field of uneven staining in the section from this tumor, which may suggest that in some microenvironments, O^6-bGua depletion is not uniform.

Temozolomide reduces MGMT content in melanoma

Alkylating chemotherapeutics which generate O^6-alkylguanine in host DNA also deplete cells of MGMT. We examined the loss of MGMT in metastatic melanoma from a patient treated with temozolomide. One subcutaneous malignant melanoma biopsy was collected from a patient with recurring metastatic melanoma. Three days later the patient was treated with temozolomide (250 mg/m^2, i.v.), and after 3 h a second single subcutaneous tumor was biospied. The tumors were sectioned and NFC2 anti-MGMT antibody staining was compared in these two samples by QIF. The untreated tumor had an average of 260 000 $\pm$ 59 000 MGMT molecules per nucleus (65 nuclei scored), whereas 3 h post-treatment MGMT content was reduced by 70% to 78 000 $\pm$ 22 000 molecules per nucleus (34 nuclei scored). MGMT-specific staining was localized in both the nucleus and

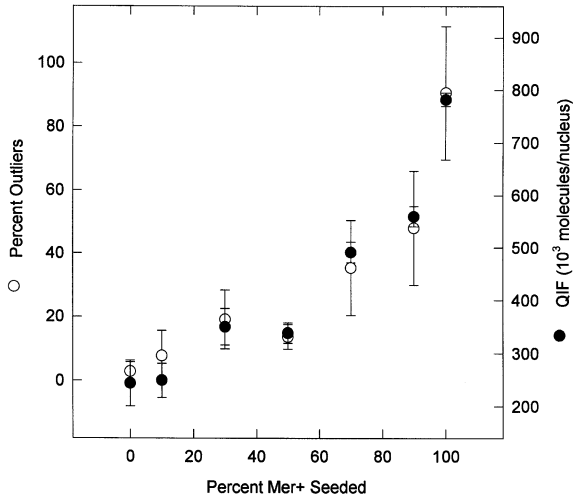

Fig. 5 Quantitative immunofluorescence of mixed populations of Mer^+ and Mer^- cells stained with M_{ab} 3B8. Cells were seeded with different proportions of Mer^+ (T98G) and Mer^- (U87MG) cells, grown overnight, stained with M_{ab} 3B8 and individual cells were assayed for MGMT content by QIF. Between 35 and 80 nuclei were scored for each point. *Abscissa* percentage Mer^+ seeded; *ordinates*: *open circles* percentage outliers (percent of cells 2.4 standard deviates greater than background fluorescence), *filled circles* average molecules per nucleus

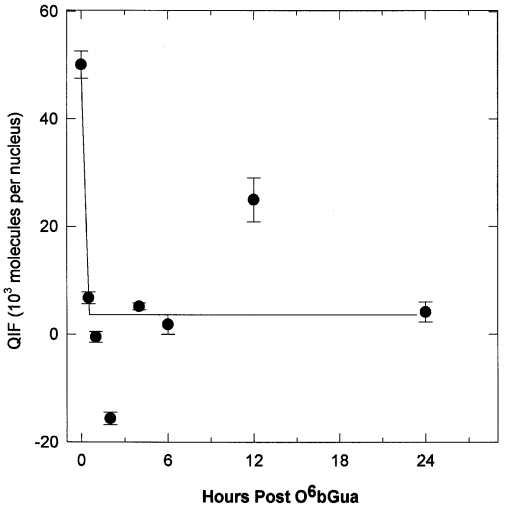

Fig. 6 QIF analysis of xenograft tumors excised from hosts after treatment with O^6-bGua (90 mg/m^2). Tumors were flash frozen in liquid nitrogen, cryosectioned, stained with M_{ab} 3B8, and quantitated by QIF. Between 67 and 211 nuclei in each section were scored

cytoplasm of untreated tumor with the majority of staining located in the cytoplasm (Fig. 7B). The treated tumor had greatly reduced staining both in the cytoplasm and the nucleus (Fig. 7D).

Discussion

MGMT confers resistance to the cytotoxicity of nitrosoureas in cell culture [11], in human xenograft [18],

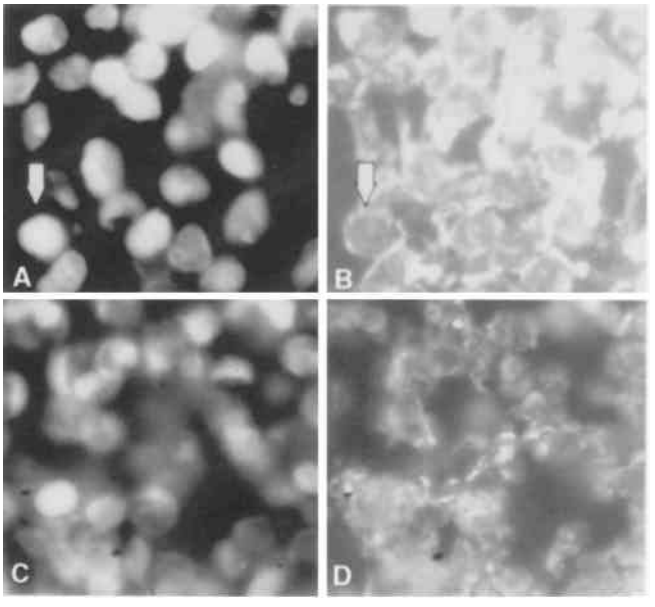

Fig. 7A–D Melanoma skin metastases stained with MGMT-specific M_{ab} NFC2 and analyzed by QIF. **A**, **B** DAPI and MGMT images of tumor excised 3 days pre-treatment. *Arrow* indicates intense cytoplasmic staining. **C**, **D** DAPI and MGMT images of tumor excised 3 h post-treatment with 250 mg/m^2 temozolomide administered as a 1 h i.v. injection

and in transgenic [9] mice, and the sensitization of tumors by the MGMT inhibitor O^6-benzylguanine further supports this mechanism of resistance [8]. The translation of this basic science to clinical application requires the measurement of MGMT in specimens of human tumors. While MGMT levels in human tumors have been surveyed by biochemical assay [5], it is widely recognized that an immunohistochemical approach is needed [16].

The antibody staining was adapted to tumor samples prepared as cryostat sections and as paraffin block sections. For laboratory studies in which the sample format can be controlled, the brightest and most clear staining is achieved when the cells are grown on coverslips or slides. This eliminates overlapping cells, and guarantees the most uniform cellular fixation and permeabilization for antibody access to all MGMT molecules. However, application of this technique to clinical specimens means that the samples are tissue pieces collected for traditional histochemical analysis. Cryostat sections are preferable to paraffin block sections since they need not be dewaxed and are less likely to suffer deformation from this additional handling. The advantage in using this technique in paraffin sections is that it opens up the use of archival material in tissue banks held at many clinical research centers. In whatever format the samples were collected, frozen storage after sectioning is important in preserving the antigen.

The immunofluorescence method described here allows MGMT quantitation in human tissue samples by digital image analysis. The QIF measurements are proportional to MGMT biochemical activity, not only by the measurement of average antibody binding in cells, but by the measure of the fraction of cells with high MGMT in a population distribution. The latter measure may be critical in evaluating tumors with mixed populations of sensitive and resistant cells.

We calibrated the fluorescence with bead standards to calculate average MGMT molecules per nucleus (Fig. 3) but the results were nearly an order of magnitude greater than the calculation using the of activity assay with a radiolabeled substrate. It is not surprising that the two methods for measuring MGMT differ as the functional specific activity of the biochemical substrate often differs from the manufacturer's reported value ([14], unpublished observations), while the bead standards themselves are calibrated in an indirect way (by absorbing them with FITC-conjugated mouse antibodies against T-cell antigens, and comparing their fluorescence to the fluorescence of similarly stained T-cells, assuming that the number of binding sites per cell are known).

In examining many cell lines and tissues with several monoclonal antibodies, we frequently observed cytoplasmic localization of MGMT. Within the same micrograph field of HT29 cells we found some cells with predominantly nuclear MGMT, while nearby cells had predominantly cytoplasmic staining. This is an unexpected finding for a DNA repair protein, and, in fact, previous studies have reported nuclear MGMT [4], with only an occasional mention of cytoplasmic staining [13]. Recently, Ishibashi *et al.* [10] found that MGMT was predominantly in the cytoplasm of HeLa S3 cells, and that MGMT must be within the nucleus to participate in repair which affected cell survival. We have confirmed the localization of MGMT in the cytoplasm of many cells by direct observation and by demonstrating antibody binding in cytoplasts of enucleated T98G glioblastoma cells. By comparing antibody staining in the enucleated cytoplasts to that in nuclei, we estimate that one-quarter to one-third of MGMT is in the cytosol in T98G cells. This is less than the value reported by Ishibashi *et al.* [10] for HeLa S3 cells and by Pegg *et al.* [17] for the non-nuclear fraction in rat liver.

It is possible that cytoplasmic MGMT appears in some but not all cells and tissues, or at some cell cycle points or at some stage of cell stress. The function of cytoplasmic MGMT is not known, nor is the mechanism for its transport into the nucleus understood. The small size of the MGMT protein and its DNA binding property may allow apparent mobilization to nuclear DNA by passive diffusion and DNA binding. We have continued to measure only nuclear MGMT in our QIF method because we have found that the nuclear MGMT measurements are proportional to the MGMT activity measurements, and for practical reasons the easy and clear outlining of the nucleus by double-staining greatly facilitates the computerized image analysis of single cells. It is often impossible in tissue sections to identify and outline all the cells of a region using a stain compatible with immunofluorescence. A greater understanding of the role of cytoplasmic MGMT may lead to new strategies in selecting whole cell or cell compartments for measurements.

The heterogeneity of MGMT expression in a cell population can only be examined using a single-cell method such as the QIF technique. In clonal populations with little or no selection (such as cell culture strains or human tumor xenografts in mice), MGMT shows a normal distribution among the cell population. In tumors, which represent clonal populations subjected to more rigorous selection, we frequently found skewed population distributions with a subpopulation of outliers from background with significantly higher MGMT content. These outliers may be of great importance since they may be the source of cells resistant to BCNU or MGMT modulators which regrow after the initial response. This possibility emphasizes that it may not be the *average* MGMT level in a tumor cell population which determines drug resistance, but the *fraction* of high-MGMT outliers which survive treatment and regrow [1].

O^6-bGua is being developed as a modulator of MGMT to sensitize tumors to alkylating agents such as BCNU and temozolomide. Benzylation of the MGMT protein alone does not lead to proteolysis, since *in vitro* reaction of O^6-bGua with purified MGMT does not block antibody binding in ELISA (nor do its most common acetylated or hydroxylated metabolites; unpublished observation), but antibody binding in immunohistochemistry is lost in O^6-bGua treated cells. In xenografts, MGMT depletion by O^6-bGua alone, as measured by QIF was rapid and prolonged, in parallel with the depletion of MGMT activity [8]. Thus, the QIF assay may be useful in monitoring the modulation of MGMT by O^6-bGua in the clinical setting. The type of MGMT depletion which might be observed is illustrated by the depletion of MGMT in subcutaneous melanoma treated with temozolomide (Fig. 7).

In summary, the antibody-based QIF assay reveals the nuclear and cytoplasmic localization and wide intercellular heterogeneity of MGMT. The assay is useful in a variety of formats, including cells spotted on slides, frozen specimens and standard paraffin sections, for measuring baseline MGMT levels and monitoring changes produced by biological sensitizers and chemotherapy. These techniques may improve the usefulness of nitrosoureas in the treatment of human cancer.

Acknowledgements Work was supported in part by National Cancer Institute grant UO1CA577-25 and contract N44-CM-27360.

References

1. Aabo K, Roed H, Vindelov L, Spang-Thomsen M (1994) A dominated and resistant subpopulation causes regrowth after response to 1, 3-bis(2-chloroethyl)-1-nitrosourea treatment of a heterogeneous small cell lung cancer xenograft in nude mice. Cancer Res 54 : 3295
2. Ayi T, Loh K, Ali R, Li B (1992) Intracellular localization of human DNA repair enzyme methylguanine-DNA methyltransferase by antibodies and its importance. Cancer Res 52 : 6423
3. Belanich M, Ayi T, LI B, Kibitel J, Grob D, Randall T, White A, Citron M, Yarosh D (1994) Analysis of O^6-methylguanine-DNA methyltransferase in individual human cells by quantitative immunofluorescence microscopy. Oncol Res 6 : 129
4. Brent T, Von Wronski M, Edwards C, Bromley M, Margison G, Rafferty J, Pegram C, Bigner D (1993) Identification of nitrosourea-resistant human rhabdomyosarcomas by in situ immunostaining of O^6-methylguanine-DNA methyltransferase. Oncol Res 5 : 1
5. Citron M, Decker R, Chen S, Schneider S, Graver M, Kleynerman L, Kahn L, White A, Schoenhaus M, Yarosh D (1991) O^6-Methylguanine-DNA methyltransferase in human normal and tumor tissue from brain, lung and ovary. Cancer Res 51 : 4131
6. Citron M, Graver M, Schoenhaus M, Chen S, Decker R, Kleynerman L, Kahn L, White A, Fornace A, Yarosh D (1992) Detection of messenger RNA from O^6-methylguanine-DNA methyltransferase gene MGMT in human normal and tumor tissues. J Natl Cancer Inst 84 : 337
7. Dolan ME, Moschel R, Pegg A (1990) Depletion of mammalian O^6-alkylguanine-DNA alkyltransferase activity by O^6benzylguanine provides a means to evaluate the role of this protein in protection against carcinogenic and therapeutic alkylating agents. Proc Natl Acad Sci USA 87 : 5368
8. Felker G, Friedman H, Dolan M, Moschel R, Schold C (1993) Treatment of subcutaneous and intracranial brain tumor xenografts with O^6-benzylguanine and 1, 3-bis(2-chloroethyl)-1-nitrosourea. Cancer Chemother Pharmacol 32 : 471
9. Gerson S, Zaidi N, Dumenco L, Allay E, Fan C, Liu L, O'Connor P (1994) Alkyltransferase transgenic mice: probes of chemical carcinogenesis. Mutat Res 307 : 541
10. Ishibashi T, Nakabeppu Y, Sekiguchi M (1994) Artificial control of nuclear translocation of DNA repair methyltransferase. J Biol Chem 269 : 7645
11. Kaina B, Fritz G, Mitra S, Coquerelle T (1991) Transfection and expression of human O^6-methylguanine-DNA methyltransferase (MGMT) cDNA in Chinese hamster cells: the role of MGMT in protection against the genotoxic effects of alkylating agents. Carcinogenesis 12 : 1857
12. Kleihues P, Burger P, Scheithauer B (1993) The new WHO classification of brain tumors. Brain Pathol 3 : 255
13. Lee SM, Harris M, Rennison J, McGown A, Bromley M, Elder R, Rafferty J, Crowther D, Margison G (1993) Expression of O^6-alkylguanine-DNA alkyltransferase *in situ* in ovarian and Hodgkins tumors. Eur J Cancer 29A : 1306
14. Major GN, Gardner EJ, Lawley PD (1991) Direct assay for O^6-methylguanine-DNA methyltransferase and comparison of detection methods for the methylated enzyme in polyacrylamide gels and electroblots. Biochem J 277 : 89
15. O'Reilly S, Newlands E, Glaser M, Brampton M, Rice-Edwards J, Illingworth R, Richards P, Kennard C, Colquhoun I, Lewis P, Stevens M (1993) Temozolomide: a new oral cytotoxic chemotherapeutic agent with promising activity against primary brain tumors. Eur J Cancer 29A : 940
16. Pegg A, Byers T (1992) Repair of DNA containing O^6-alkylguanine. FASEB J 6 : 2302
17. Pegg A, Wiest L, Foote R, Mitra S, Perry W (1983) Purification and properties of O^6-methylguanine-DNA transmethylase from rat liver. J Biol Chem 258 : 2327
18. Schold SC, Brent TP, Von Hofe E, Friedman HS, Mitra S, Bigner DD, Swenberg JA, Kleihues P (1989) O^6-Alkylguanine-DNA alkyltransferase and sensitivity to procarbazine in human brain-tumor xenografts. J Neurosurg 70 : 573
19. Yarosh DB (1991) Purification and administration of DNA repair enzymes. US Patent 5077211, 31 December
20. Yarosh D, Fornace A, Day R (1985) Human O^6-alkylguanine-DNA alkyltransferase fails to repair O^4-methylthymine and methyl phosphotriesters in DNA as efficiently as does the alkyltransferase from *Escherichia coli*. *Carcinogenesis* 7: 949